Analysis of air quality observations with the aid of the source–receptor relationship approach

Marina Astitha[a], George Kallos[a*], Nikos Mihalopoulos[b]

[a] *University of Athens, School of Physics, University Campus, Bldg PHYS-5, 15784 Athens, Greece*

[b] *Environmental Chemical Process Laboratory, Department of Chemistry, University of Crete, P.O Box 1470, 71409, Heraklion, Greece*

[*]**Corresponding author**. National & Kapodistrian University of Athens, Department of Applied Physics, Laboratory of Meteorology, University Campus, Bldg PHYS -V, Athens 15784, Greece
Tel. +30-210-7276835, Fax. +30-210-7276765
E-mail: kallos@mg.uoa.gr

Abstract

In this study an attempt was made to analyze time series of air quality measurements (O_3, SO_2, SO_4^{2-}, NO_x) conducted at a remote place in the Eastern Mediterranean (Finokalia at Crete Island in 1999) to obtain concrete information on potential contributions from emission sources. For the definition of a source-receptor relationship, advanced meteorological and dispersion models appropriate to identify "areas of influence" have been used. The model tools used are the advanced atmospheric modeling system RAMS and a Lagrangian-type particle dispersion model-LPDM (forward and backward in time) with capabilities to derive influence functions and definition of "areas of influence". When high levels of pollutants have been measured at the remote location of Finokalia, particles are released from this location (receptor) and they are traced backward in time. The influence function derived from particle distributions characterizes dispersion conditions in the atmosphere and also provide information on potential contributions from emission sources within the modeling domain to this high concentration. As it was shown in the results from the simulations, the experimental site of Finokalia in Crete is influenced during the selected case studies, primarily by pollutants emitted from the urban conglomerate of Athens. Secondarily is influenced by polluted air masses arriving from Italy and/or the Black Sea Region. For some specific cases air pollutants monitored at Finokalia were possibly related to war activities in the West Balkan Region (Kossovo).

***Keywords**:* Air quality measurements; influence function; modeling, source-receptor relationship; impact assessment

INTRODUCTION

Measurements of conventional air pollutants such as O_3, SO_2, SO_4^{2-}, NO_x, black carbon, in specific locations provide the basic information on the air quality at local and regional scale. When levels of high pollutants cannot be sufficiently interpreted by taking into account local emission sources, emphasis is given on the study of long range transport of pollutants to the areas of interest. Meteorological and air quality models are very useful tools for the interpretation of air quality measurements and the verification of the reasons leading to increased air pollutant concentration in the remote areas of the world [1,2,3].

The identification of sources influencing the air quality over a specific area is performed with the aid of dispersion models. In this paper a Lagrangian dispersion model is used in combination with a regional atmospheric model. The key factor of choosing this method is the ability to perform simulations backward in time, starting from specific areas that are considered as receptors of possible transport of pollutants from remote locations. This method in contrast with the well known simulation forward in time can be used as a tool for investigating the possible origin of air masses, when a long range transport is most likely to have occurred. In that manner such simulation can offer a great assistance in the interpretation of measurements of high pollutant concentration in specific areas. The performance of simulations backward in time with a dispersion model combined with an atmospheric model, offers an opportunity to identify the origin of air masses influencing the air quality of a certain receptor area.

The main purpose of this study is the analysis of available air quality measurements at a remote location using the source-receptor relationship approach, through the combined use of two arithmetic models, the Regional Atmospheric Modeling System (RAMS) and the Lagrangian Particle Dispersion Model (LPDM- with the implementation of turbulent diffusion), to evaluate the long range transport influencing this location. Measurements have been provided by the Environmental Chemical Processes Laboratory (ECPL), Department of Chemistry, at University of Crete, from the air quality station of Finokalia, located in a coastal area. No major emission sources of air pollution exist in the greater area around the station.

A brief description of the models used in this study follows, as well as a description of the method used for the performance of the measurements of specific pollutants. In addition, the configuration of the simulations is presented focusing on the input data used for each simulation. The results from the simulations are discussed thoroughly, focusing on some case studies on spring 1999.

DATA AND MODELS USED

Air Quality Measurements

O_3, aerosol and other gaseous pollutants measurements (SO_2, NO_x), have been conducted at Finokalia (35º30'N, 25º70'E) located 70 Km East-Northeast of Heraklion, at the northern coast of Crete (Figure 1). The station is located at the top of a hilly elevation (150 m) facing the sea within the sector of 270˚ to 90˚. The nearest village has less than 10 inhabitants and it is situated at a distance of 3 km to the south of the station. No tourist or other types of human activities occur at a distance shorter than 20 km within the above mentioned sector. The remoteness of the Finokalia station and its representativity of its measurements on regional basis have been demonstrated in a number of articles published up to day. Below a short overview will be given:

- NO and NO_2 are monitored using a Thermo Environmental Model 42C high sensitivity chemiluminescence instrument with detection limit of 50pptv[4]. Long-term measurements (more than 6 years) at Finokalia show that NO levels (a pollutant clearly indicating local and/or regional anthropogenic influence form combustion, traffic etc) has a range between the detection limit (most of the time) and 100 pptv. The highest levels always occur during sunrise and can be explained by photochemical conversion of NO_2 to NO, indicating thus absence of any local source of combustion close to the station.

- At Finokalia, ozone measurements are made by using a Dasibi 1080 AH analyzer[4]. The long-term measurements of O_3 at Finokalia (from 1997 today) point out (i) the existence of a well defined seasonal cycle with maximum during summer months, (ii) the presence of elevated O_3 levels (up to 80 ppbv) during summer-time and over time-periods of several days, (iii) the absence of any important diurnal cycle indicating that local photochemistry has a rather weak impact on O_3 levels[4, 5, 6].

-During a 14-month period O_3 concentrations have been simultaneously monitored at Finokalia and onboard of the passenger vessel “El Greco” traveling in the Aegean Sea in the S-N direction. A total of 120 round-trips have been performed and the observed O_3 concentrations ranged from 10 to 93 ppbv (average 50 ± 8 ppbv). The O_3 levels observed above the Aegean Sea are comparable to those measured at Finokalia at the NE coast of Crete during the same period (51 ± 8.5 ppbv), indicating that the O_3 observations at the monitoring station of Finokalia are representative of the regional background in the Eastern Mediterranean.

-Measurements of black carbon have been performed at Finokalia using a PSAP analyzer (Particle Scattering Absorption Photometer). Measurements of black carbon using this technique have been successfully compared with the results obtained using the thermo-optical determination technique[7].

-Bulk aerosols were collected on open face 0.45 μm Gelman Zefluor PTFE filters placed on the same mast with the inlets of O_3 and NOx. Using a flow rate of 1.45 m^3h^{-1}, the mean sampling interval varied between 3 and 48 hours. Filter analysis was conducted in the laboratory using ion chromatography. A Dionex AS4A-SC column with ASRS-I suppressor in auto suppression mode of operation was used for the analysis of SO_4^{2-}. The measured mean nss-SO_4^{2-} concentration is among the highest reported for rural areas in Europe. The highest concentrations are associated with transport from Western and Central Europe and occur during the dry period when dry deposition is the main removal mechanism for aerosol particles[6].

More detail about the station and the meteorological conditions encountered in this area are given in [4, 5, 6].

Model Description

Regional Atmospheric Modeling System – RAMS

RAMS is a highly versatile numerical code developed by scientists at Colorado State University and ASTER, Inc. for simulating and forecasting meteorological phenomena [8, 9, 10]. It is considered as one of the most advanced modeling systems available today. It has been developed in order to simulate atmospheric phenomena with resolution ranging from tens of kilometers to a few meters. There is no lower limit to the domain size or to the mesh cell size of the model finite difference grid. A general description of the model and its capabilities is given in [9, 10]. However, over the most important features of RAMS is the use of a two-way interactive nesting with any number of either telescoping or parallel fine nest grids, terrain following coordinate surfaces with Cartesian or polar stereographic horizontal coordinates, the use of non-hydrostatic or hydrostatic time-split time differencing. RAMS also performs cloud microphysics parameterization at various levels of complexity, uses various turbulence parameterization schemes, radiative transfer parameterizations (short and long wave) through clear and cloudy atmospheres. Various options are used for upper and lateral boundary conditions and for finite operators, various levels of complexity for surface-layer parameterization (soil model, vegetation etc.). European Centre for Medium-Range Weather Forecasts (ECMWF) and National Center for Environmental Predictions (NCEP) analysis files can also be used for initialization. In general, RAMS is a highly versatile tool that can be used in air quality studies and in a wide variety of other atmospheric phenomena.

Lagrangian Particle Dispersion Model - LPDM

The LPDM is a simulation tool to investigate atmospheric flow and pollution dispersion over complex terrain for domains up to several hundred kilometers. It is based on the work performed by Marek Uliasz [11, 12] initially. Further development was performed at University of Athens, by the Atmospheric Modeling and Weather Forecasting Group. The LPDM allows one to simulate releases of pollution from arbitrary emission sources by tracking the motion of particles.

The unique feature of the LPDM is its ability to use two different options for dispersion modeling: the source-oriented and the receptor–oriented mode. The traditional source-oriented approach consists in solving dispersion model equations forward in time for given sources of pollutant. As a result a time- and space-dependent concentration field C is obtained. In order to investigate another emission scenario the solution of the model equations must be repeated.

In many practical applications, air pollution at a given receptor is of primary interest and the alternative receptor oriented modeling should be considered as a more effective approach. Air quality at the receptor is characterized by an integral of pollution concentration over the modeling domain and time of simulation. In the receptor-oriented modeling method an influence function C^* is determined instead of concentration. The influence function can be calculated from backward trajectories of particles or puffs when Lagrangian dispersion models are used. If Eulerian models are used, the influence function is obtained as a solution of adjoint equations backward in time with the receptor function as a source term. The influence function calculated for a given receptor depends on meteorology and transformation of pollutant in the atmosphere but is independent of emission sources. Receptor-oriented modeling is especially relevant to such applications as emission control, planning locations of new emission sources and assessing contributions from different sources to air pollution in a given area.

The LPDM model uses the meteorological fields (wind, potential temperature, turbulent kinetic energy) calculated by RAMS. The LPDM and the receptor-oriented approach in dispersion modeling are discussed in more detail in Uliasz [11, 12].

Model Configuration

The simulations with RAMS discussed in this paper were performed for three selected periods during 1999. The selection was based on the dates where high pollutant concentrations were measured in the areas characterized as receptors of air pollution. The first simulation was performed for the period March 28 to April 2, 1999. The second period is April 6 to 9, 1999 and the third is April 27 to 29, 1999. During spring of 1999, war operations in Kossovo of the 'Allied Force' have been performed. Under selected days during that period very high values of ozone and sulfate were measured in Finokalia station (compared to the long-term measurements available for this area and period of time).

The main purpose of implementing a Lagrangian dispersion model is to identify the origin of air masses that influence the air quality of a receptor area and thus to examine if any relation between the increased values and the war operations exist. Previous work[13] showed evidence of pollution transport in Balkans during the war operations. The performance of a simulation backward in time with the dispersion model provides the identification of temporal and spatial origin of air masses ending up at the receptor area.

A nested grid configuration was implemented, with the coarse grid covering the greater Mediterranean Area and one finer telescoping grid covering Greece, as shown in Figure 1. The coarse grid has a mesh of 113x61 points and 48 km horizontal grid increment; the coordinates of the center of the domain were 39,0^{o}N and 20,0^{o} E. The finer grid has a mesh of 152x164 points and 8km horizontal grid increment; the coordinates of the center of the domain were 37,5^{o} N, 24,5^{o}E. In the vertical, 31 vertical layers of variable resolution were applied. The vertical structure was denser in the lower levels while it became increasingly coarser toward the top of the model domain. For initial and lateral boundary conditions the 0.5x0.5 degrees latitude-longitude gridded analysis dataset of ECMWF was used with time increment of 6 hours. The original topography dataset is from United States Geological Survey (USGS) with resolution of 30x30 arc seconds. Similar dataset from the same origin was used for vegetation coverage and land-use.

CASE STUDIES

Case Study 1: March 28 – April 2, 1999

During the period of March 28 to April 2, 1999, high sulfate aerosol and black carbon concentration (Figure 2a, b) but low O_3 levels (Figure 7a) were measured at Finokalia station compared to the seasonal average[4, 6]. The synoptic conditions prevailing in the area during the period under investigation are characterized mainly by a high pressure system covering the Central Mediterranean, traveling NE by the end of March. A high pressure system appears at April 2 in Western Mediterranean traveling east, affecting the Ionian Sea and the island of Crete. At the upper atmosphere a trough over Northern Mediterranean Area weakly affects the area. The low pressure system over Northern Aegean at March 28 weakens through the next days, and high pressure system affects the area. The near surface (z=43m) wind fields for selected and representative hours are illustrated in Figure 3. Model output evaluation showed a quite good agreement with observations from the World Meteorological Organization (WMO) network. This evaluation is a standard procedure that is beyond the scope of the present work and is not included here.

The duration of the dispersion simulations was either two or five days according to the strength of the horizontal component of transport and the origin of the air masses. When the air masses were outside the domain under consideration or from locations with no major sources, the simulation was terminated. The influence function calculations indicate the areas where the air masses were located at the time intervals indicated. For example, when we present simulations starting at 12:00UTC (Figure 4) with a time interval of 6 hours, the reader should interpret the figures as follows: The first frame starting from the top left indicates where the monitored masses were located during the previous 6 hours, meaning 12:00-6:00UTC, April 2,

1999. The second frame on top line indicates where the air masses were located during the time increment between 0:00-6:00UTC, April 2, 1999. That means 6 to 12 hours before they were monitored at Finokalia station. The third frame of the top line indicates the position of the monitored air masses during the time increment of 0:00-18:00UTC of the previous day. That means 12-18 hours before the sampling time. The same way the simulation continues up to the time increment of 114-120 hours. It must be clearly stated that the figures indicate the position of the air masses (and therefore the existence or not of various-type of sources) and not the concentration or apportionments of pollutants monitored.

The first simulation started on April 2, 1999, at 12:00UTC, continued for 5 days backwards in time, considering the station at Finokalia as the receptor area. The date is chosen for the analysis of a high concentration value of particulate sulfate measured at Finokalia station for that period of year[6], as shown in Figure 2a (denoted with a white dot). The air masses ending up at Finokalia at that specific date are located in the maritime area west of Crete during the last 24hr (Figure 4). Looking at 36 to 40 hours backwards in time (00:00 and 06:00 UTC, 1/4/1999), the air masses are traveling through the greater Athens area as well as western Greece. In that point the air masses are divided into two different paths. The first path, looking back in time for 3 days is located in NW Turkey, Black Sea SE Bulgaria. The second smaller path comes from the area of Ionian Sea and West Balkan Region. Results from the atmospheric model showed strong NE flow for April 30 and 31, in the area of northern Aegean Sea, which weakens the next day. On April 2 appears a strong western flow pattern in the area west of Crete Island.

The second simulation started on April 1, 1999, at 00:00UTC and continued for 4 days backwards in time, considering Finokalia as the receptor area (Figure 5). The simulation is performed for the analysis of the second peak of sulfate during that period, as shown in Figure 2a (denoted with a white square). The air masses located at Finokalia for the starting date, 24hr backwards in time (31/3, 00:00UTC) were located in the Adriatic Sea while 48hr backwards in time (30/3, 00:0UTC) are traced in Western Balkans. 3 to 4 days backwards in time the air masses were located outside the modeling domain. War operations in Kossovo during the operation ‘Allied Force’ as recorded in several publications[14], included bombing of aircraft factory and household appliances factory in central Serbia (Cacak, Pancevo) at March 29 and 30, 1999. The wind flow pattern calculated by the RAMS model showed significant north-northwest flow in the maritime area of western Greece, leading the air masses towards western Crete and the area of Finokalia station in a time scale of about 12hr.

The third simulation of this case study started on March 31, 1999, at 12:00UTC, with Finokalia station being the receptor area. This date was chosen due to the peak value of black carbon concentration measured at Finokalia (Figure 2b). The influence function calculated (Figure 6) exhibits a similar pattern as the one described in Figure 5 for the first two days of the simulation. The pattern changes as we move backwards in time, where 72hr before (28/3, 12:00UTC), the air masses are located at the west part of Greece, having a major influence from southern Italy and the Adriatic Sea.

In the first case study, during the period March – April 1999, the measurements of air pollutants from Finokalia (receptor) are possibly related to certain source areas through long range transport of air masses. Possible source area is the city of Heraklion in a short time scale (about 6hours), and the coastal areas of Ionian and Adriatic Sea in a longer time scale (about 36hours) when west, northwest flow dominates in the area (Figures 5-6). Another flow pattern influencing the receptor area at Finokalia is the northern flow pattern, where air masses are traveling through the Aegean Sea, ending up in Finokalia (Figure 4). In several cases the air masses are traveling through the greater Athens area before they arrive in northern Crete (Figures 4, 9). Such flow pattern is predominant in the area mostly in the summer, due to the appearance of Etesians (strong northern flow) in the Aegean Sea. In several simulations the well known flow pattern from the Black Sea and Bulgaria becomes evident, affecting the areas chosen as receptors in this study.

Case Study 2: April 6 – April 9, 1999

During this period measurements of ozone concentration exhibit a peak value for two days, reaching 80ppb approximately (Figure 7). Simulations with the dispersion model in combination with the atmospheric model were performed for the selected period April 6 to 9, 1999.

The synoptic conditions during this time of the year are characterized mainly by a high pressure system in the area of Eastern Mediterranean, which remains in the area until April 9. On April 7, a cold front of a trough moving northeast affects Greece. At the surface weak wind flow of western direction is the main pattern in the area, developing local circulations due to the physiographic characteristics in each region. The wind flow pattern described above is clearly indicated from the RAMS simulations (Figure 8).

The first simulation with the dispersion model started on April 8, 1999, at 12:00UTC, and continued for 48hr backwards in time, considering Finokalia as the receptor area. The influence function as shown in Figure 9 provides with a clear image of the traveling path of the air masses ending up at Finokalia at the desired time. Each frame represents a 6hr interval. It becomes evident that the air masses were located in the greater Athens area during the past 12hr, while 36hr before (April 7, 1999, 6:00UTC) a part of the air masses is located in the area of western Balkans and the second one in the area of Albania. Possible sources of influence of the air masses are considered: the target-areas of war operations in Kossovo [15](reports on bombing in fuel storage in Pristina and in central storage depot in Novi Sad at April 7, 2:40LST, and in chemical industry in central Serbia at April 6, 20:35LST). Another possible source is considered the greater Athens area and Adriatic Sea since the air masses remain in the area for almost 24hr. The results from RAMS model clearly indicate the northwest flow which seems to act in a very catalytic way upon the movement of the air masses.

The second simulation of this case study is performed for the analysis of the second peak of ozone during the period of April 6-9, 1999 (Figure 10). The simulation started on April 9, 1999 at 12:00UTC, continued for 48hr backwards in time, considering Finokalia as the receptor area. 24hr earlier, the air masses are located west of Crete Island, while looking back 42hr the air masses are located south, in the maritime area near Libya. There is no connection with the war operations in Kossovo, while it is considered possible that the peak of ozone has its origin in the area of Heraklion, west of Finokalia when west winds are prevailing in the area at this time. At this point it is useful to mention the differences appearing in the traveling path of the air masses when they travel through land or sea. In the first simulation the landscape variability has a major influence in the movement of the air masses as expected. In the second simulation the air masses are traveling all the way in the maritime area, where the stable marine boundary leads to the smooth movement of the air masses during the 48hr of the simulation period.

In certain case studies of this work, appears a well indicated flow pattern of the air masses through the area of Kossovo and central Serbia, in a time scale of 48 to 72 hours before they are traced in Crete (Figure 9). When these dates coincide with war operations in Yugoslavia, with possible emission of pollutants capable of long range transport, there can be a relationship between the war operations and the pollutant measurements in the receptor areas. Further proof of such relation, needs a detailed examination of wet and dry deposition covering the entire traveling path of the air masses, as well as the contribution of a photochemical model for the accurate simulation of the chemical reactions and transformation of the pollutants in the atmosphere.

Case Study 3: April 27 – April 29, 1999.

The third case study focuses on the analysis of a peak concentration of ozone measured at Finokalia station on April 28, 1999 (Figure 11). The synoptic conditions during this period of the year are characterized mainly by the passage of a trough in Western Europe, with its eastern part being above northern Italy during April 27. A second trough is located in Eastern Mediterranean, influencing the Aegean Sea, but weakens until April 29. Then the Aegean Sea is mainly influenced by the first trough which has moved southeast at the time. At the surface there is the presence of a depression at April 27, moving east through west Italy, and at April 29 the cold front of the depression is located above western Greece.

The synoptic conditions mentioned above, lead to the appearance of certain wind flow patterns in the area of the Aegean Sea. Such patterns are well demonstrated with the aid of the atmospheric model RAMS. On April 27, at 12:00UTC a weak north-northwest flow is evident at central and south Aegean Sea, which turns to south-southeast for the next 6hr (Figure 12a). During the next day appears a strong northwest flow prevailing in the area of NW Aegean Sea and Crete Island (Figure 12b).

The simulation with the dispersion model started on April 28, 1999, at 22:00UTC, and continued for 43hr backwards in time considering Finokalia as the receptor area. The air masses are located in Bulgaria and near the Dardanelles gat looking back 43hr in time, as evident in Figure 13. They were transferred south, along the Aegean Sea and were traced finally at Finokalia. The air masses when entering Northern Aegean Sea stayed in the area for about 30hr, due to the light winds prevailing in the area. When reaching central Aegean Sea at April 28, the air masses are influenced by a northwest flow, which guides them to the Island of Crete. There is no significant vertical transport during the travel of the air masses, except when sea-land distribution forces them to move upwards or downwards.

CONCLUSIONS

During this study an attempt was made to analyze air quality measurements from a remote station at Finokalia, Crete. The time series available covered a period of two years continuous measurements (1999 and 2000) and simulations were performed for all the available measurements. Paths and scales of transport during the warm period of the year have been studied extensively in the past for the area of East Mediterranean [16, 17]. In this paper the analysis is focusing on spring cases because dispersion and transport patterns are more complicated. Several other cases during other seasons of the year have been also performed but either the patterns are well known from existing publications [16, 17] or are during rainy episodes where the washout effects are not included in this version of the dispersion model.

The simulations with the dispersion model are performed for time periods of 2 to 5 days backwards in time to account for the possible long range transport of air masses. There is an evident relationship between air masses traveling through Greece and those coming from the Balkan Region, Eastern Europe and Central Mediterranean Region. Such relation is always relevant with the prevailing atmospheric conditions in the area.

The determination of the transport pattern of air masses from remote locations and the identification of the areas of origin both in space and time was gained with the use of the modeling approach. It was also possible to verify the characteristic transport paths and scales of air masses in space and time for the specific time of the year. This was feasible due to the inclusion of turbulent diffusion in the dispersion model. There are clear differences in the results of such model in conjunction with the simple back trajectory models, where turbulence is not taken under consideration. The results of these simulations are considered as more accurate, concerning the movement of air masses in the atmosphere.

This modeling approach in combination with a photochemical model and high frequency pollutants measurements, can contribute in the management of various sources affecting the air quality of area(s) of interest. It can assist also in the impact assessment of various hazardous environmental incidents.

Acknowledgements

The authors of this paper acknowledge the support from the EU (DG XII and DG Research) projects SUBAERO (EKV2-1999-00052), ADIOS (EVK3-CT-2000-00035) and MERCYMS (EVK3-2002-00070). We would like to thank the anonymous reviewers for their constructive comments and suggestions.

References

1. Luria M., M. Peleg, G. Sharf, D. Siman Tov-Alper, N. Schpitz, Y. Ben Ami, Z. Gawi, B. Lifschitz, A. Yitzchaki, and I. Seter, 1996: Atmospheric Sulphur over the East Mediterranean region. J. Geophys. Res., 101, 25917-25930.
2. Kallos, G., V. Kotroni, K. Lagouvardos, and A. Papadopoulos, 1999: "On the transport of air pollutants from Europe to North Africa". Geophysical Research Letters. 25, No 5, 619-622.
3. Kotroni V., Kallos G., Lagouvardos K., Varinou M., 1999, "Numerical simulations of the Meteorological and Dispersion conditions during an Air Pollution Episode over Athens, Greece", J. of Applied Meteorology, Vol.38, p432-447.
4. Kouvarakis G., Tsigaridis, K., Kanakidou, M., and Mihalopoulos, N., Temporal variations of surface regional background ozone over Crete Island in southeast Mediterranean, *J. Geophys. Res.,* 2000, *105*, 4399-4407.
5. Mihalopoulos N., Stephanou, E., Kanakidou, M., Pilitsidis, S., and Bousquet, P., Tropospheric aerosol ionic composition above the Eastern Mediterranean Area, *Tellus B,* 314-326, 1997.
6. Kouvarakis G., and N. Mihalopoulos, Seasonal variation of dimethylsulfide in the gas phase and of methanesulfonate and non-sea-salt sulfate in the aerosol phase measured in the Eastern Mediterranean atmosphere, Atmos. Environ., 36, 929-938, 2002.
7. Bardouki H., Liakakou H., Economou C., Smolic J., Zdimal V., Eleftheriadis K., Lazaridis M., and N. Mihalopoulos, 2003. Chemical composition of Size

Resolved Atmospheric Aerosols in the Eastern Mediterranean During Summer and Winter. Atmospheric Environment, 37, 195-208.

8. Walko, R. L., and C. J. Tremback, 1996: RAMS - *The Regional Atmospheric Modelling System Version 3b: User's Guide*. Published by ASTeR, Inc., PO Box 466, Fort Collins, Colorado, 86 pp.

9. Pielke, R.A., W.R. Cotton, R.L. Walko, C.J. Tremback, W.A. Lyons, L.D. Grasso, M.E. Nicholls, M.D. Moran, D.A.Wesley,T.J. Lee, and J.H. Copeland, 1992: A comprehensive meteorological modeling system - RAMS. Meteorol. Atmos. Phys. 49, 69-91.

10. Cotton, W.R.; Pielke Sr., R.A.; Walko, R.L.; Liston, G.E.; Tremback, C.J.; Jiang, H.; McAnelly, R.L.; Harrington, J.Y.; Nicholls, M.E.; Carrio, G.G.; McFadden, J.P., 2003, "*RAMS 2001: Current Status and Future Directions",* Meteorology and Atmospheric Physics, Springer-Verlag, Vol 82, Issue 1-4.

11. Uliasz M., Pielke R., "Application of the receptor oriented approach in mesoscale dispersion modeling", Proc. Of the 18th NATO/CCMS Int. Techn. Meeting on Air Pollution Modeling and its Applications, edited by H. van Dop and D.G. Steyn, Plenum Press, NY 1990, Vancouver, Canada, Vol.2, p 401.

12. Uliasz M., 1993, "The Atmospheric Mesoscale Dispersion Modeling System", Journal of Applied Meteorology, Vol.32 , Pp139-149.

13. Melas, D., Zerefos, C., Rapsomanikis S., Tsangas N., Alexandropoulou A., 2000. The war in Kossovo. Evidence of pollution transport in the Balkans during Operation Allied Force. Environmental Science & Pollution Research 7, 97-103.

14. UNEP/UNCHS, Balkans Task Force (BTF), 1999. The Kossovo Conflict. Consequences for the Environment and Human Settlements, Geneva.

15. Vukmirovic Z., Unkasevic M., Lazic L., Tosic I., 2001, "Regional air pollution caused by a simultaneous destruction of major industrial sources in a war zone. The case of Serbia in April 1999." Atm. Environment, Vol35, 2773-2782.

16. Kallos, G., and P. Kassomenos, 1993: Effects of the selected domain in mesoscale atmospheric simulations and dispersion calculations. Proc. of the 20th ITM of NATO/CCMS on Air Pollution Modeling and its Application. November 29 - December 3, 1993. Valencia, Spain. Edited by Sven-Erik Gryning and Millan M. Millan, Plenum Press, X, pp. 35-44

17. Kallos G., V. Kotroni, K. Lagouvardos, M. Varinou, and A. Papadopoulos, 1995: "Possible mechanisms for long range transport in the eastern Mediterranean" Proc.

of the 21st NATO/CCMS Int. Techn. Meeting on Air Pollution Modeling and Its Application, 6-10 November, Baltimore, USA. Edited by S Gryning and F. Schiermeier, Plenum Press, New York, Vol 21, pp.99-107.

<u>Figure 1</u>: a) Grid configuration for the simulation period of March, April 1999. **b)** Location of the measuring site at Finokalia, Crete.

<u>Figure 2:</u> a) Measurements of particulate sulfate SO_4^{-2} at the station of Finokalia for the period March – April 1999. **b)** Measurements of black carbon at the station of Finokalia for the period March – April 1999. The hours indicate local time.

<u>Figure 3</u>: Temperature (contours) and wind field (arrows) at 43.7m above sea level, on **a)** March 28, 1999, at 12:00UTC, **b)** March 29, 1999, at 12:00UTC, **c)** March 30, 1999, at 12:00UTC, **d)** March 31, 1999, at 12:00UTC, **e)** April 1, 1999, at 12:00UTC, **f)** April 2, 1999, at 12:00UTC**.**

<u>Figure 4</u>: Influence function calculated for 5 days backwards in time, starting on April 2, 1999, at 12:00UTC. Receptor = Finokalia (35,32^o E, 25,67^o N). Each frame presents a 6hr interval. The sequence is from top left to bottom right.

<u>Figure 5</u>: Influence function calculated for 4 days backwards in time, starting on April 1, 1999, at 00:00UTC. Receptor = Finokalia (35,32^o E, 25,67^o N). Each frame presents a 6hr interval. The sequence is from top left to bottom right.

<u>Figure 6</u>: Influence function calculated for 84hrs backwards in time, starting on March 31, 1999, at 12:00UTC. Receptor = Finokalia (35,32^o E, 25,67^o N). Each frame presents a 6hr interval. The sequence is from top left to bottom right.

<u>Figure 7:</u> a) Ozone measurements at Finokalia station, for April 1999. (UTC=LST-3h). b) Ozone measurements at Finokalia station, for April 8, 1999. c) Ozone measurements at Finokalia station, for April 9, 1999.

<u>Figure 8:</u> Temperature (contours) and wind field (arrows) at 43.7m above sea level, on a) April 7, 1999, at 00:00UTC, b) April 8, 1999, at 12:00UTC, c) April 9, 1999, at 00:00UTC.

<u>Figure 9</u>: Influence function calculated for 48hrs backwards in time, starting on April 8, 1999, at 12:00UTC. Receptor = Finokalia (35,32^o E, 25,67^o N). Each frame presents a 6hr interval. The sequence is from top left to bottom right.

<u>Figure 10</u>: Influence function calculated for 48hrs backwards in time, starting on April 9, 1999, at 12:00UTC. Receptor = Finokalia (35,32^o E, 25,67^o N). Each frame presents a 6hr interval. The sequence is from top left to bottom right.

<u>Figure 11:</u> Ozone measurements at Finokalia station, for April 29, 1999.

<u>Figure 12:</u> Temperature (contours) and wind field (arrows) at 43.7m above sea level on a) April 27, 1999, at 12:00UTC and b) April 28, 1999, at 12:00UTC.

Figure 13: Influence function calculated for 43hrs backwards in time, starting on April 28, 1999, at 22:00UTC. Receptor = Finokalia (35,32° E, 25,67° N). Each frame presents a 6hr interval. The sequence is from top left to bottom right.

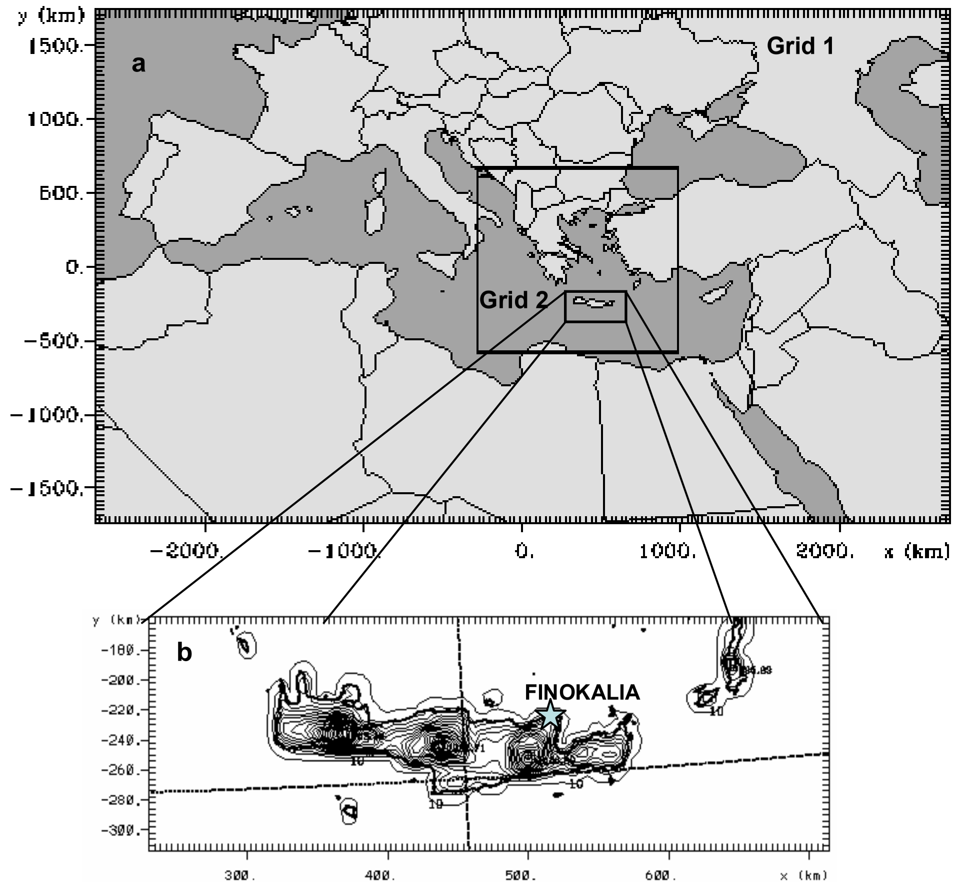
a
Grid 1
Grid 2
y (km)
x (km)
b
FINOKALIA

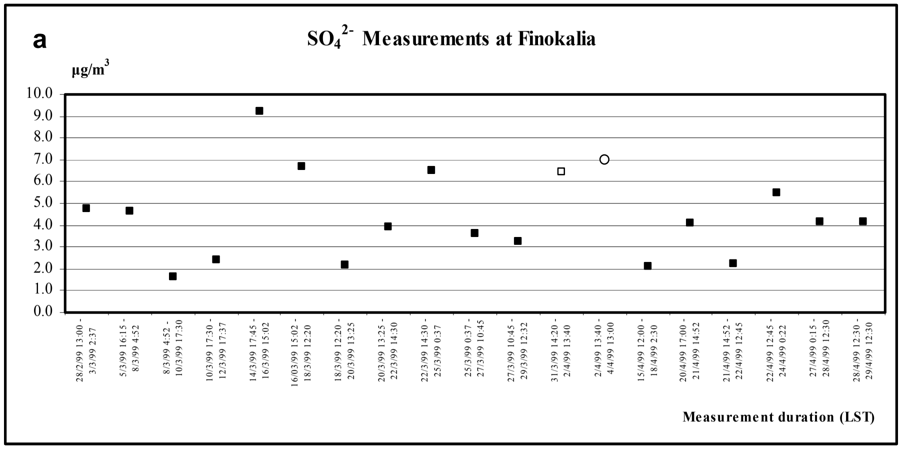
a
SO4 2- Measurements at Finokalia
µg/m3
Measurement duration (LST)

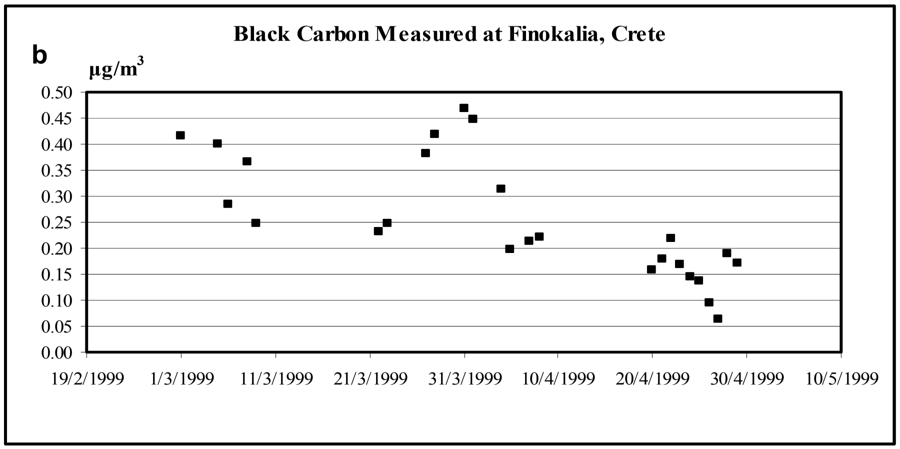
Black Carbon Measured at Finokalia, Crete
b
µg/m3
19/2/1999
1/3/1999
11/3/1999
21/3/1999
31/3/1999
10/4/1999
20/4/1999
30/4/1999
10/5/1999

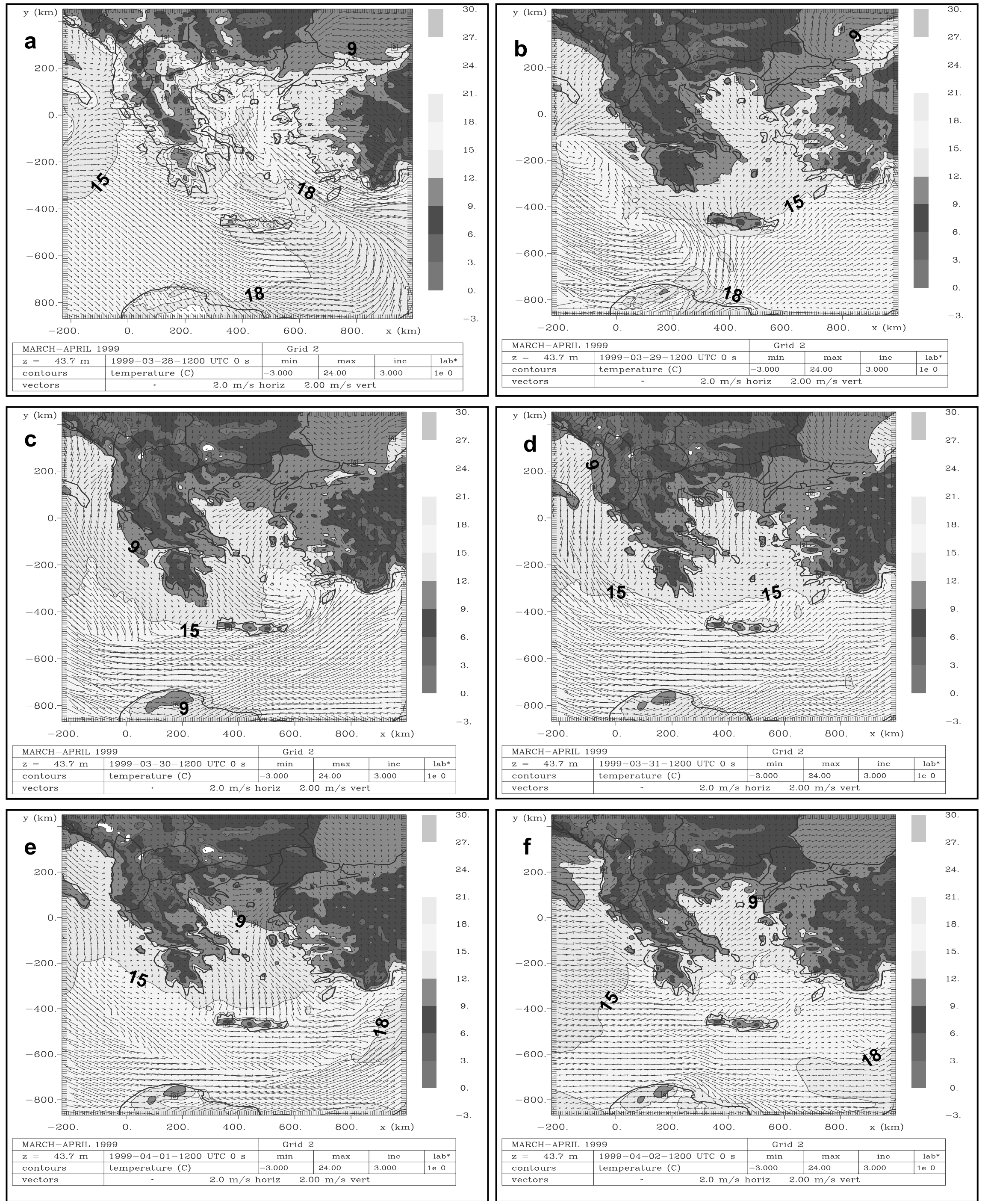
a
b
c
d
e
f
y (km)
x (km)
MARCH–APRIL 1999
Grid 2
z = 43.7 m
1999-03-28-1200 UTC 0 s
1999-03-29-1200 UTC 0 s
1999-03-30-1200 UTC 0 s
1999-03-31-1200 UTC 0 s
1999-04-01-1200 UTC 0 s
1999-04-02-1200 UTC 0 s
min
max
inc
lab*
contours
temperature (C)
-3.000
24.00
3.000
1e 0
vectors
2.0 m/s horiz
2.00 m/s vert

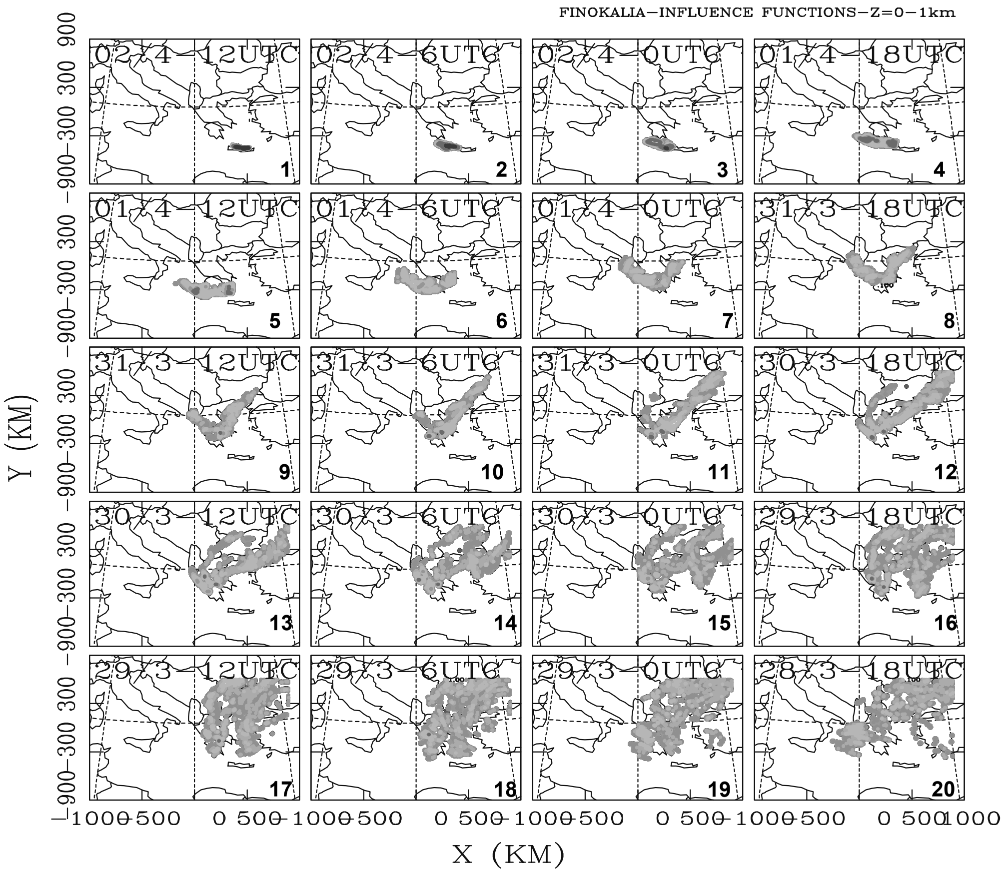

FINOKALIA–INFLUENCE FUNCTIONS–Z=0–1km
02/4–12UTC
02/4–6UTC
02/4–0UTC
01/4–18UTC
01/4–12UTC
01/4–6UTC
01/4–0UTC
31/3–18UTC
31/3–12UTC
31/3–6UTC
31/3–0UTC
30/3–18UTC
30/3–12UTC
30/3–6UTC
30/3–0UTC
29/3–18UTC
29/3–12UTC
29/3–6UTC
29/3–0UTC
28/3–18UTC
1
2
3
4
5
6
7
8
9
10
11
12
13
14
15
16
17
18
19
20
Y (KM)
X (KM)

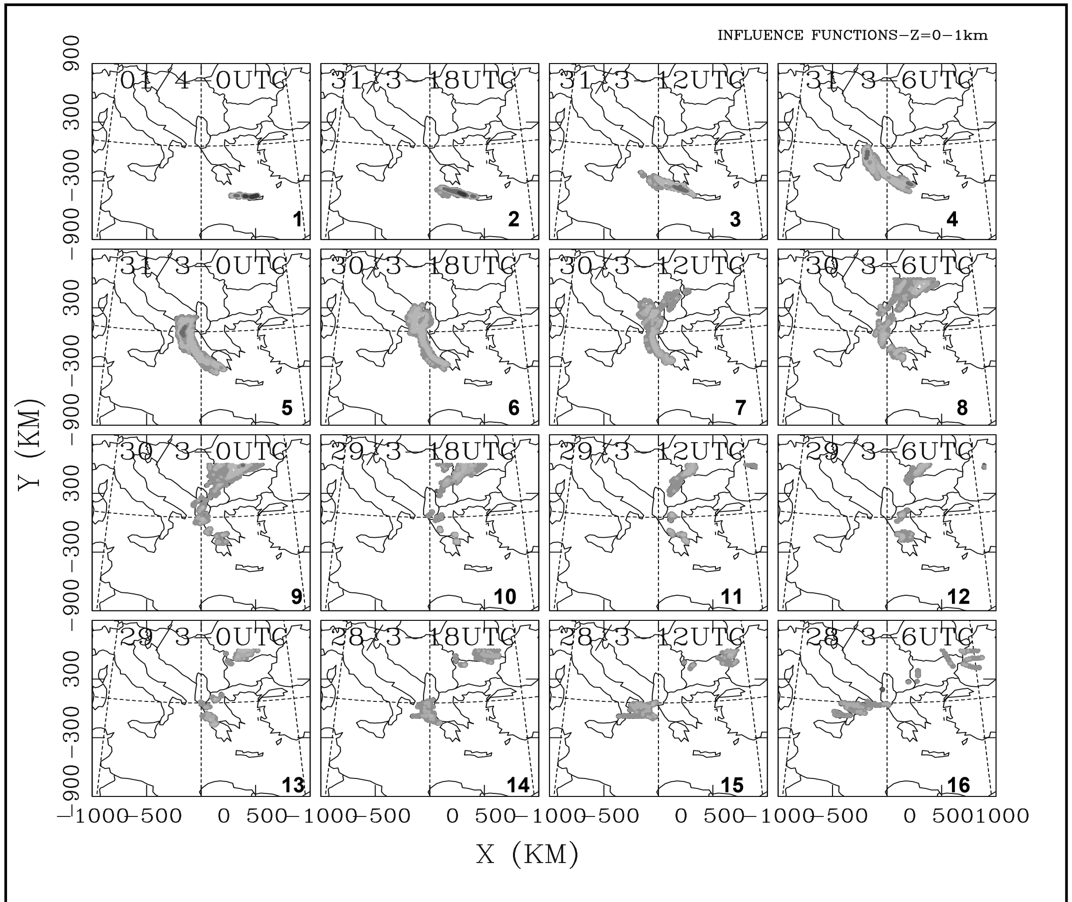
INFLUENCE FUNCTIONS-Z=0-1km
01/4-0UTC
31/3-18UTC
31/3-12UTC
31/3-6UTC
31/3-0UTC
30/3-18UTC
30/3-12UTC
30/3-6UTC
30/3-0UTC
29/3-18UTC
29/3-12UTC
29/3-6UTC
29/3-0UTC
28/3-18UTC
28/3-12UTC
28/3-6UTC
1
2
3
4
5
6
7
8
9
10
11
12
13
14
15
16
Y (KM)
X (KM)

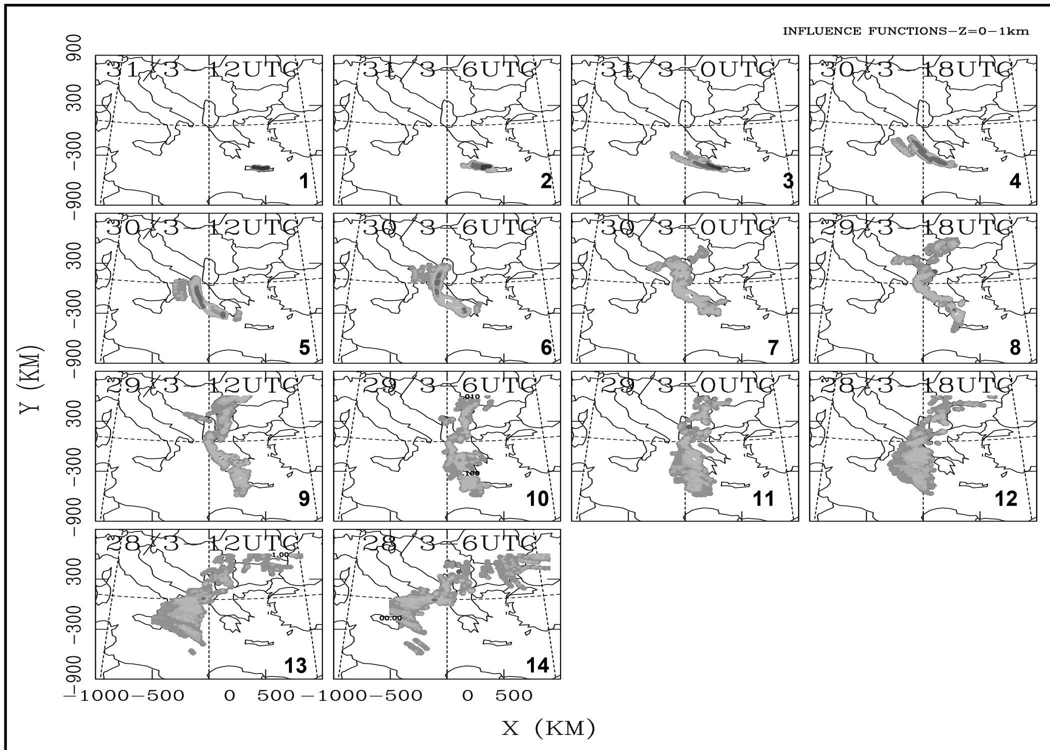
INFLUENCE FUNCTIONS–Z=0–1km
31/3–12UTC
31/3–6UTC
31/3–0UTC
30/3–18UTC
30/3–12UTC
30/3–6UTC
30/3–0UTC
29/3–18UTC
29/3–12UTC
29/3–6UTC
29/3–0UTC
28/3–18UTC
28/3–12UTC
28/3–6UTC
1
2
3
4
5
6
7
8
9
10
11
12
13
14
Y (KM)
X (KM)

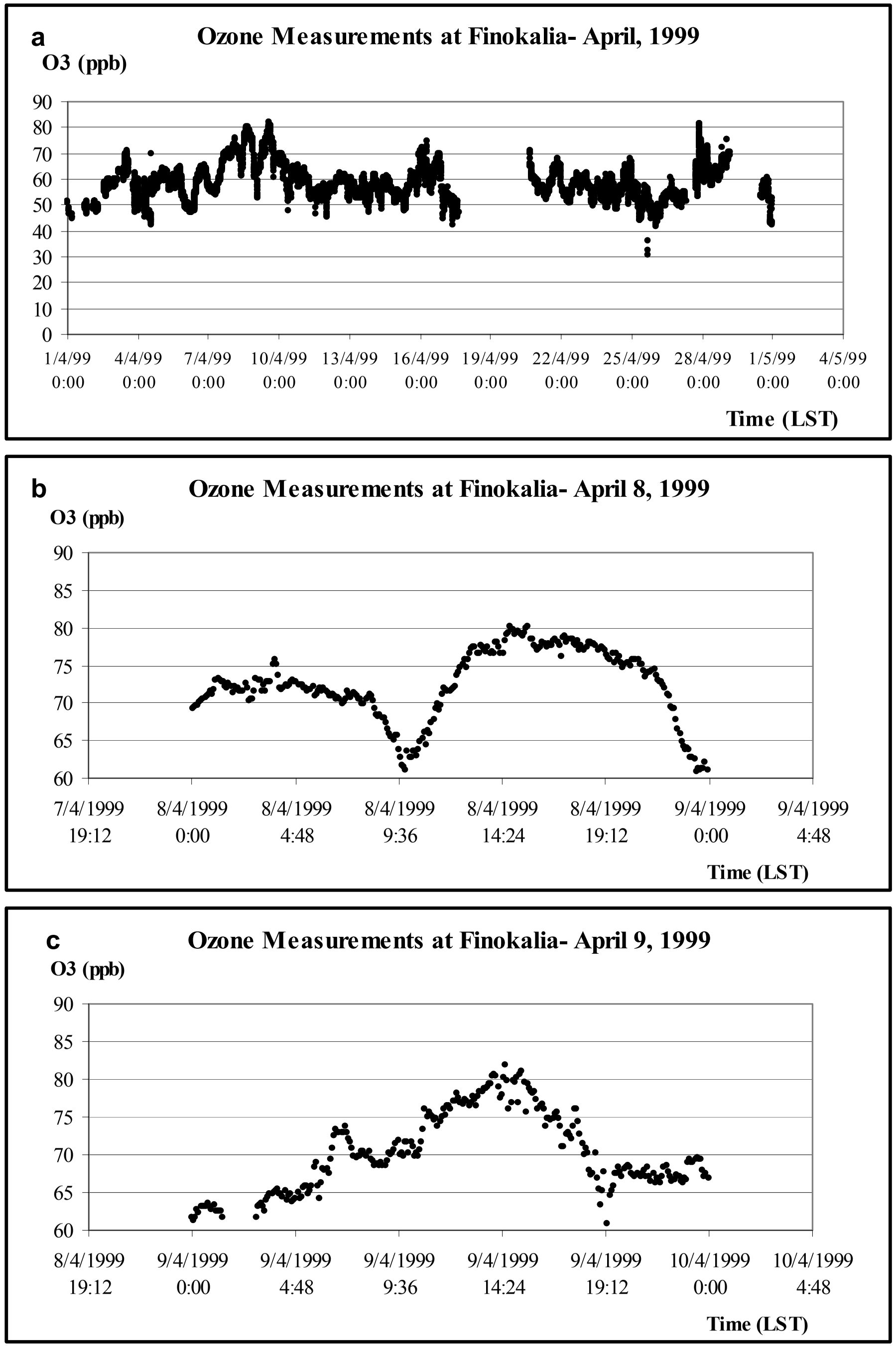
a
Ozone Measurements at Finokalia- April, 1999
O3 (ppb)
90
80
70
60
50
40
30
20
10
0
1/4/99 0:00
4/4/99 0:00
7/4/99 0:00
10/4/99 0:00
13/4/99 0:00
16/4/99 0:00
19/4/99 0:00
22/4/99 0:00
25/4/99 0:00
28/4/99 0:00
1/5/99 0:00
4/5/99 0:00
Time (LST)
b
Ozone Measurements at Finokalia- April 8, 1999
O3 (ppb)
90
85
80
75
70
65
60
7/4/1999 19:12
8/4/1999 0:00
8/4/1999 4:48
8/4/1999 9:36
8/4/1999 14:24
8/4/1999 19:12
9/4/1999 0:00
9/4/1999 4:48
Time (LST)
c
Ozone Measurements at Finokalia- April 9, 1999
O3 (ppb)
90
85
80
75
70
65
60
8/4/1999 19:12
9/4/1999 0:00
9/4/1999 4:48
9/4/1999 9:36
9/4/1999 14:24
9/4/1999 19:12
10/4/1999 0:00
10/4/1999 4:48
Time (LST)

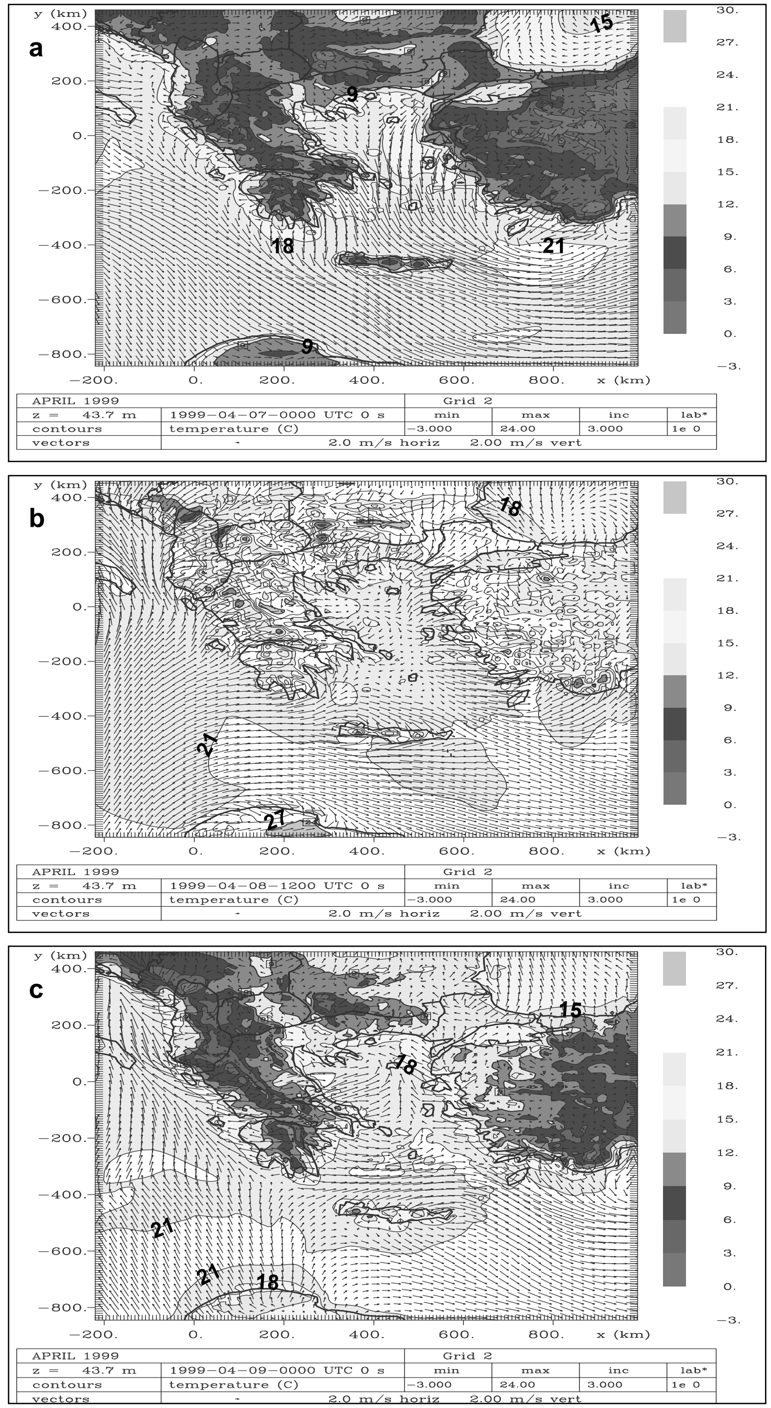
a
b
c
y (km)
x (km)
APRIL 1999
Grid 2
z = 43.7 m
1999-04-07-0000 UTC 0 s
1999-04-08-1200 UTC 0 s
1999-04-09-0000 UTC 0 s
min max inc lab*
contours
temperature (C)
-3.000 24.00 3.000 1e 0
vectors
2.0 m/s horiz 2.00 m/s vert

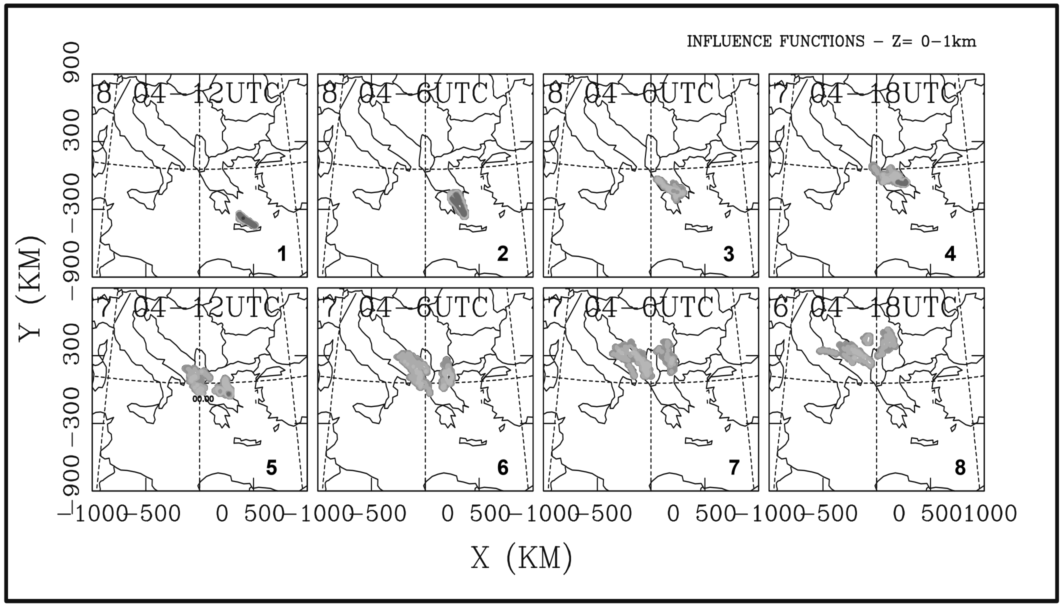
INFLUENCE FUNCTIONS - Z= 0-1km
8/04-12UTC
8/04-6UTC
8/04-0UTC
7/04-18UTC
7/04-12UTC
7/04-6UTC
7/04-0UTC
6/04-18UTC
1
2
3
4
5
6
7
8
Y (KM)
X (KM)

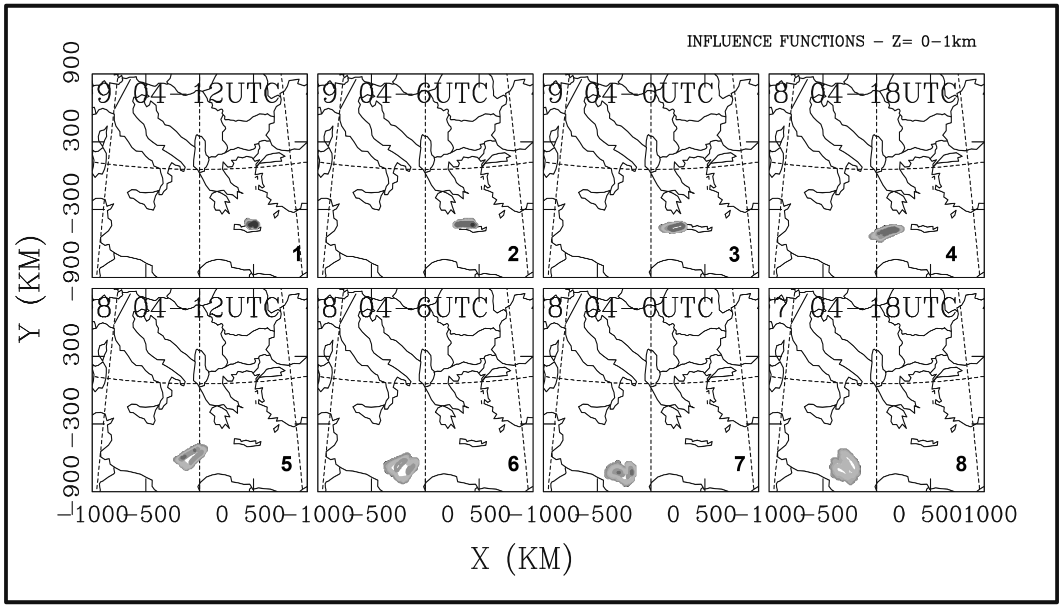
INFLUENCE FUNCTIONS – Z= 0–1km
9/04–12UTC
9/04–6UTC
9/04–0UTC
8/04–18UTC
8/04–12UTC
8/04–6UTC
8/04–0UTC
7/04–18UTC
1
2
3
4
5
6
7
8
Y (KM)
X (KM)
900
300
–300
–900
–1000
–500
0
500
1000

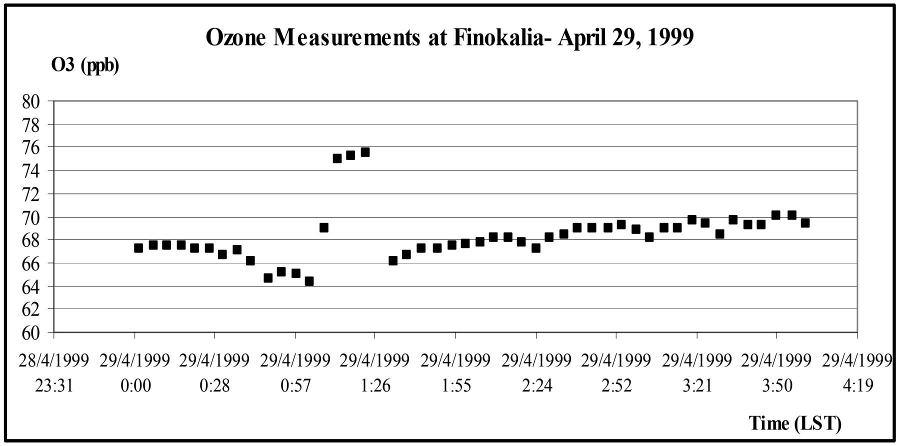
Ozone Measurements at Finokalia- April 29, 1999
O3 (ppb)
80
78
76
74
72
70
68
66
64
62
60
28/4/1999 23:31
29/4/1999 0:00
29/4/1999 0:28
29/4/1999 0:57
29/4/1999 1:26
29/4/1999 1:55
29/4/1999 2:24
29/4/1999 2:52
29/4/1999 3:21
29/4/1999 3:50
29/4/1999 4:19
Time (LST)

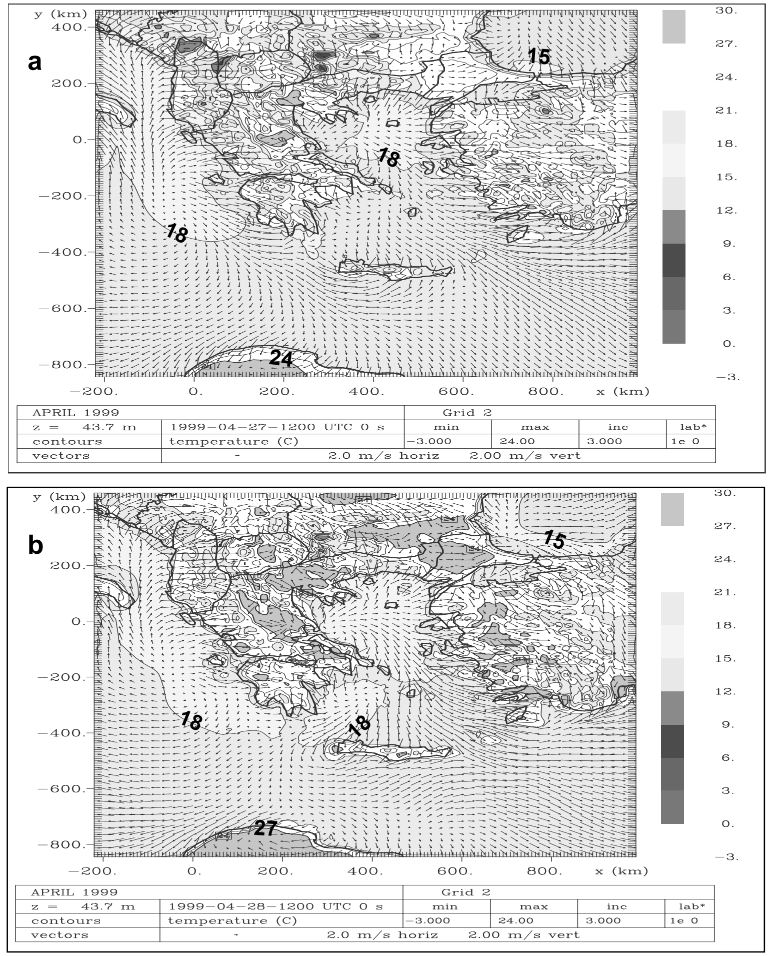
a
y (km)
400.
200.
0.
−200.
−400.
−600.
−800.
−200.
0.
200.
400.
600.
800.
x (km)
15
18
18
24
30.
27.
24.
21.
18.
15.
12.
9.
6.
3.
0.
−3.
APRIL 1999
Grid 2
z = 43.7 m
1999−04−27−1200 UTC 0 s
min
max
inc
lab*
contours
temperature (C)
−3.000
24.00
3.000
1e 0
vectors
-
2.0 m/s horiz
2.00 m/s vert
b
y (km)
400.
200.
0.
−200.
−400.
−600.
−800.
−200.
0.
200.
400.
600.
800.
x (km)
15
18
18
27
30.
27.
24.
21.
18.
15.
12.
9.
6.
3.
0.
−3.
APRIL 1999
Grid 2
z = 43.7 m
1999−04−28−1200 UTC 0 s
min
max
inc
lab*
contours
temperature (C)
−3.000
24.00
3.000
1e 0
vectors
-
2.0 m/s horiz
2.00 m/s vert

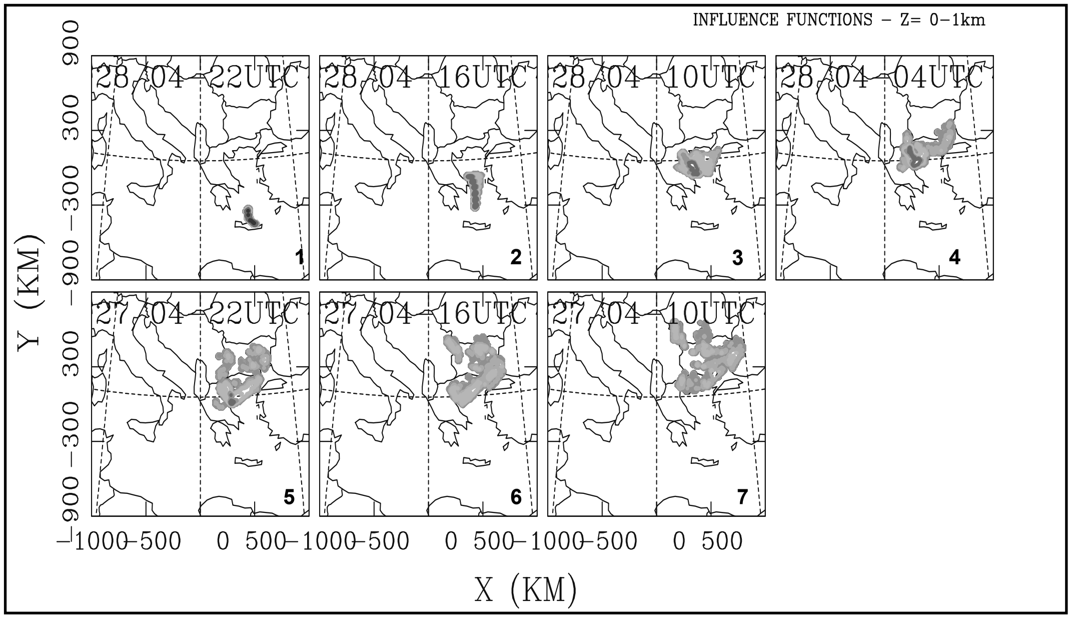
INFLUENCE FUNCTIONS – Z= 0–1km
28/04–22UTC
1
28/04–16UTC
2
28/04–10UTC
3
28/04–04UTC
4
27/04–22UTC
5
27/04–16UTC
6
27/04–10UTC
7
Y (KM)
X (KM)